Hindawi
Wireless Communications and Mobile Computing
Volume 2022, Article ID 5089078, 10 pages
https://doi.org/10.1155/2022/5089078

Research Article

A Novel CNN-Inception-V4-Based Hybrid Approach for Classification of Breast Cancer in Mammogram Images

Muhammad Saquib Nazir,[1] Usman Ghani Khan ,[1] Aqsa Mohiyuddin,[2] Mana Saleh Al Reshan,[3] Asadullah Shaikh ,[3] Muhammad Rizwan,[4] and Monika Davidekova[5]

[1]*Department of Computer Science, University of Engineering and Technology, Lahore 54890, Pakistan*
[2]*Department of Computer Science, Kinnaird College for Women, Lahore 54890, Pakistan*
[3]*College of Computer Science and Information Systems, Najran University, Najran 61441, Saudi Arabia*
[4]*Secure Cyber Systems Research Group, WMG, University of Warwick, Coventry CV4 7AL, UK*
[5]*Information Systems Department Faculty of Management, Comenius University in Bratislava, Odbojárov 10, 82005 Bratislava 25, Slovakia*

Correspondence should be addressed to Usman Ghani Khan; usman.ghani@kics.edu.pk

Received 30 April 2022; Revised 13 June 2022; Accepted 18 June 2022; Published 6 July 2022

Academic Editor: Kuruva Lakshmanna

Breast cancer is the most frequent disease in women, with one in every 19 women at risk. Breast cancer is the fifth leading cause of cancer death in women around the world. The most effective and efficient technique of controlling cancer development is early identification. Mammography helps in the early detection of cancer, which saves lives. Many studies conducted various tests to categorize the tumor and obtained positive findings. However, there are certain limits. Mass categorization in mammography is still a problem, although it is critical in aiding radiologists in establishing correct diagnoses. The purpose of this study is to develop a unique hybrid technique to identify breast cancer mass pictures as benign or malignant. The combination of two networks helps accelerate the categorization process. This study proposes a novel-based hybrid approach, CNN-Inception-V4, based on the fusing of these two networks. Mass images are used in this research from the CBIS-DDSM dataset. 450 images are taken for benign, and 450 images are used for malignant. The images are first cleaned by removing pectoral muscles, labels, and white borders. Then, CLAHE is used to these images to improve their quality in order to produce promising classification results. Following preprocessing, our model classifies cancer in mammography pictures as benign or malignant abnormalities. Our proposed model's accuracy is 99.2%, with sensitivity of 99.8%, specificity of 96.3%, and F1-score of 97%. We also compared our proposed model to CNN, Inception-V4, and ResNet-50. Our proposed model outperforms existing classification models, according to the results.

1. Introduction

Breast cancer becomes one of the most serious diseases and leading causes of mortality in women worldwide [1]. Breast cancer develops when aberrant cells in the breast proliferate excessively [2]. Breast cancer is classified into two types: benign and malignant. Benign is treatable, but it can become hazardous over time. Malignant is perilous [3]. It has the potential to spread to other organs of the body and cause death. In developed countries, the proportion of cancer cases is growing. This is a major issue in healthcare. As a result, early identification of breast cancer can lower the risk of patient death [4].

Mammography is indeed the good diagnostic imaging technique for detecting breast problems early on [5]. Cancer mortality rates could rise by 50% to 15 million by 2030, according to World Health Organization (WHO) predictions. Developing countries account for over 70% of new cancer cases. X-ray scans of each breast are acquired from two perspectives during a mammography screening. Human readers, such as an expert radiologist, assess and examine screening mammograms [6]. Dual reading was discovered to enhance evaluation results and has been implemented in many countries. Repeated readings with up to ten readers can boost diagnostic performance even further. Beyond the dual reading, there is much of room for improvement in mammography grading.

Based on the invasive phase of the breast anomaly, the irregularities may be benign or malignant. Detecting lumps in breast tissue is more difficult than detecting microcalcification. Many industrialised countries are adopting the smart cities concept in the modern era [7]. All of that in a smart city is controlled by a computer. Every industry in the world is moving toward the computer. Humans want computers to rule everything. In a smart city environment, decision-making is a significant difficulty [8]. This present era is sometimes referred to as the data world. Because consumers contribute data on a daily basis. This information is quite beneficial in terms of making the environment smarter. Data-driven decision AI (artificial intelligence) [9, 10] enables computers to make decisions. Data must be available to the computer in order for it to make conclusions.

Healthcare is a major global challenge [11–15]. The use of computers, smart systems, and intelligent devices is critical in healthcare. The diagnosis of sickness at an early stage can save lives [16, 17]. New breakthroughs have the potential to lessen the risk to human life [18].

Computer-Aided Diagnosis (CAD) [19] systems are used to assist radiologists in the detection and diagnosis of cancer. CAD systems have been shown in studies to be useful; yet, accurate breast cancer detection remains a difficult issue [20]. Because of the intricacy of mammography and the large number of tests performed by radiologist, incorrect diagnoses occur. The CAD system attempts to reduce incorrect diagnoses, which in turn reduces unneeded biopsies, patient anxiety, increased healthcare costs, and superfluous review by radiologists. Moving beyond traditional machine learning (ML) [21, 22], current efforts have focused on the application of deep learning (DL) approaches [22–24]. Through statistical analysis, they are able to more correctly diagnose suspected lesions. DL models are intended for huge and diverse datasets (for example, the ImageNet dataset [25]), whereas mammography contains tiny datasets that are publically available. As a result, when learning from the start with minimal training samples, the capability and complexity of such networks might have a considerable negative impact on simulation results.

Many researchers played an important role in the classification of mass images of breast cancer as benign and malignant, but still, mass classification in mammography remains a significant issue, yet it is essential in assisting radiologists in making accurate diagnoses [26]. There is also a need for such a system that can speed up the process of classification of tumors with good results, and this is possible with a unique hybrid technique. So, using the CBIS-DDSM (Curated Breast Imaging Subset of DDSM) dataset [27], this research provides a novel hybrid approach CNN-Inception-V4 for classifying breast cancer as benign or malignant. The paper's main contributions are based on the following points.

(i) To propose such a unique strategy for properly classifying breast cancer

(ii) To propose a hybrid technique that can speed up the process of breast cancer classification along with good results

(iii) To perform techniques such as image preprocessing, data augmentation, and hyperparameters (e.g., batch size, learning rate), which are appealing choices for reducing overfitting and enhancing model generalization

(iv) To compare our model to existing state-of-the-art networks

The other sections of the research are organized in the following manner: related work is done in Section 2, the proposed method and dataset used are described in Section 3, the classification results are evaluated in Section 4, and the conclusions are presented in the last section.

2. Related Work

Many researchers used various strategies to reach promising findings. The authors in [28] employed computer vision techniques to help a radiologist evaluate mammography images and diagnose a malignancy in an acceptable amount of time. They extracted various characteristics from the mammogram's selected area, which the surgeon subjectively labeled. These characteristics are supplied into a classification engine, which is then used to train and construct the suggested architecture classification models. The classification procedure by either SVM or NB with its optimum parameters resulted in 100% accuracy for the classification process. The authors in [29] proposed Fisher linear discrimination analysis (FLDA) and quadratic discrimination assessment (QDA) inside random projection (RP) filtration to evaluate our performance and efficiency with SVM classifier (SVM), K-nearest neighbour (KNN), and multilayer perceptron (MLP) in IoT-based platforms. The modelling results demonstrate not only increased accuracy but also decreased duration. In our chosen dataset simulated for a relation to health and safety, runtime is reduced by 20 times when compared to SVM, KNN, and MLP in QDA and FLDA. At the IoT business, RP filtering in the preprocessing step of feature extraction, which fulfils the model's runtime, is a point of view.

The authors in [30] proposed Blockchain-Integrated Remote Database (BIRD) paradigm that connects blockchain to a Relational Database Management System (RDBMS) that employs the Remote Database Access (RDA) protocol and a Cloud Server. This report gives a comprehensive history of blockchain and industry generations. Finally, this research proposes a next-generation blockchain architecture in which a smart government linked to Industry 4.0 monitors price increases and fraud.

The authors in [31] proposed synchronization technique based on AI to address smart grid timing difficulties. Backpropagation neural networks are used as an AI technology that utilizes time approximations and error corrections for exact results. In order to link the external time server, the unique AIFS system considers radio communication features. The suggested AIFS scheme's performance is tested using a MATLAB-based simulation technique. The simulation results suggest that the proposed approach outperforms the present system.

The authors in [27] proposed a modified network of YOLOv5 to detect and categorize breast cancers. The process was carried out with an 8-batch size, an activation function of 0.01, a velocity of 0.843, and an interval value of 300. To evaluate the suggested effectiveness of the algorithm, it is contrasted to YOLOv3 and a faster RCNN, with 93.50% MCC value and 96.50% accuracy. The suggested model beats YOLOv3 and quicker RCNN. The results show that the proposed prediction model detects and diagnoses breast tumors while also addressing previous researchers' limitations by decreasing the FPR and FNR and raising the MCC value.

The authors in [32] proposed an efficient, lightweight encryption method to provide a safe picture encryption approach for the healthcare business. To protect medical pictures, the proposed lightweight encryption solution uses two permutation algorithms. In terms of security and execution time, the suggested approach is investigated, assessed, and then compared to commonly encrypted ones. Several test photos were utilized to evaluate the proposed algorithm's performance. Several studies demonstrate that the suggested algorithm for picture cryptosystems is more efficient than existing techniques.

The authors in [33] present a study of deep learning-based load forecasting strategies from 2015 to 2020. This study addresses research in the load forecasting process that uses deep learning techniques, Distributed Deep Learning (DDL) techniques, backpropagation- (BP-) based works, and non-BP-based works. Following the survey, it was concluded that data aggregation dependence would be advantageous for lowering computing time in load forecasting. As a result, a conceptual model of DDL for smart grids has been provided, with the HSIC (Hilbert-Schmidt Independence Criterion) bottleneck approach integrated to give more accuracy.

The authors in [32] offer an experimental analysis of cryptographic algorithms in order to categorize encryption methods as symmetric or asymmetric. It provides a thorough examination of AES, DES, 3DES, RSA, and Blowfish in terms of time complexity, size, encryption, and decryption performance. The simulation technique was used for the evaluation, and the speed of encryption and decryption of the chosen encryption algorithms was examined. The experiments ran the same encryption using the same plaintext five times for each encryption and decryption, and the average time is compared. Each encryption algorithm's key size is the maximum number of bytes that the cypher may accept. The average time taken by the three devices to compute the method is utilized for comparison. In the simulation for the experimental test, a set of plaintexts—password-sized text and paragraph-sized text—achieves goal fair outcomes when compared to the existing methods in real-time deep learning networks for IoT applications.

The authors in [34] presented a model for breast cancer categorization, using the CAD technique. MIAS and DDSM datasets are used in this study. Preprocessing, categorization, gathering, and operation grouping are all used in this system. The CAD system includes a CNN model with eight coevolutionary, 4 max pooling, and two totally connected layers. The obtained findings are compared to AlexNet and VGG16, demonstrating that the suggested CNN [35] beat both of these models in terms of accuracy and AUC. The suggested model achieved accuracies of 92.54%, 96.47%, and 95% for MIAS, DDSM, and the self-collected dataset, respectively.

The authors in [36] developed an intelligent system that included picture normalization, microcalcification detection, and mammogram categorization. The best classification accuracy of the system in distinguishing between benign and malignant breasts can reach 0.8124 on the training set and 0.7237 on the test set, with an area under curve (AUC) of receiver operating characteristic of 0.8042. The sensitivity of malignant breast prediction is 0.8891 on the training dataset and 0.7778 on the testing dataset. The highest accuracy was 0.7511 on the microcalcification lesion degree, with an AUC of 0.7627 on the testing dataset.

The authors in [37] proposed a strategy to categorize breast invasive cancer using AGAN for data augmentation and CNN for tumor categorization. In many visual recognition applications, deep CNN models and other predictive analysis and ML algorithms have outperformed the state of the art. This method produced 89.17% accurate results but a 19.41% true alarm rate of classification.

The authors in [38] investigated the achievement of three types of ML methods: (1) NB, (2) NN, and (3) SVM. SVM delivers the most satisfactory results in correctly characterising the condition of the breast as "Good" or "Malignant," with a reliability of 99.4% in training and 98.76% in testing, according to the outcomes of ten experiments. In the study, the SVM classifier outperformed the NN and NB models, suggesting that SVM is an appropriate choice for assessing the state of the breast at a preliminary phase.

The authors in [39] proposed a method to identify breast tumor utilizing two deep learning model networks, Res-Net-50 and VGG-16 using the IRMA dataset and then comparing their outcomes. They attained an accuracy of 94% for VGG-16 and 91.7% for Res-Net50, as well as a sensitivity of 94% for VGG-16 and 94% for Res-Net50. Their restriction is that for VGG16 and Res-Net50, their accuracy value lowers to 89% and 88%, respectively.

The authors in [40] proposed a hierarchical twitter sentiment model (HTSM) to show people's opinions in short texts. The suggested model's quality is confirmed by applying it to a popular product and a widely discussed issue. The findings reveal that the suggested model beats state-of-the-art approaches for successfully evaluating people's opinions in brief text.

The authors in [41] provide a novel CNN structure for classifying histopathological cancer pictures that integrates spectral characteristics acquired via a multiresolution wavelet technique with CNN spatial features. Furthermore, batch normalization is employed after each layer in the convolution network to solve CNN's poor convergence problem, and CNN's deep layers are trained with spectral–spatial data. Using the BreaKHis dataset and the Breast Cancer Classification Challenge 2015 dataset, the suggested structure is evaluated on malignant histology pictures of the breast for both binary and multiclass tissue classifications. Experiment findings suggest that combining spectral–spatial data enhances CNN network classification accuracy and needs fewer training parameters than well-known models. On both datasets, the suggested structure achieves an average accuracy of 97.58% and 97.45% with 7.6 million training parameters.

The authors in [42] describe how the VGG16 framework of DL methodology was used to categorize breast cancer in mammography. The VGG16 classifier is constructed and tested using 322 photographs from the MIAS dataset. It beats the models AlexNet, EfficientNet, and GoogleNet. The categorization of mammograms will improve mammography screening effectiveness and act as a valuable mechanism for surgeons. The authors in [43] promptly made available breast cancer diagnoses at a preliminary phase of malignancy. The authors in [44] employed quicker R-CNN to identify abnormalities in mammograms to categorize masses into benign and malignant.

The authors in [45] utilize image fragmentation and limited preprocessing methods to classify cancer. In semantic segmentation, binarization is used to compare the edge detection strategy to the RCNN methodology. The authors in [46] employed a standard diversity CNN and then incorporated two improvement techniques: (i) batch normalization (BN) and (ii) drop-outs (DO). They employed rank-based stochastic pooling. As a consequence, BDR-CNN was developed, which is a hybrid of CNN, BN, DO, and RSP. This BDR-CNN was hybridised with a GCN to create our BDR-CNN-GCN framework, which was then deployed as a data augmentation strategy for breast mammography assessment. The authors in [47] explained HRD, a combination model of a radial basis function network with DT. This approach was evaluated versus three prominent algorithms: kNN, NB, and SVM. The observations reveal that their recommended technique achieved a high level of precision. The authors in [48] created a collection with chaotic tags or corrupted data and contrasted AlexNet against GoogleNet (GN) for cancer identification. The proportion of chaotic training pictures was changed to control the equilibrium of their system' memory and cognitive.

The authors in [49] developed a unique hybrid optimal feature selection (HOFS) approach to figure out the relevant characteristics to achieve maximum efficiency for this classification. To train the neural network, a number of carefully chosen characteristics are used. In this proposed technique, the searchable relevant information from the minimammographic data capture organization (MIAS) collection was included. The authors in [50] develop a framework for assessing cancer in mammograms. Chroma noise, fragmentation, and clustering are among the phases in the suggested model. The image enhancement is used to improve the image quality from digital mammograms. The term "fuzzy" refers to the employment of a clustering algorithm to segment a breast tumor. The Bi-LSTM method generates EHO to diagnose cancer with performance characteristics. In this study, the MIAS dataset is employed. The results are then contrasted to CNN and DCNN, as well as Bi-LSTM, with EHOBi-LSTM beating everyone else, although FPR and FNR levels need to be decreased. The authors in [51] suggested that system is a combination stages: pretreatment and development of a Convolution Neural Network (CNN). The preparation process sets the mammograms data for the CNN building phase, which encompasses format unity, denoising, image enhancement, ROI retrieval, augmentation, and image scaling. In the CNN development phase, the proposed CNN model is built from the ground up in addition to learning features and identify tumor progression in mammograms data.

According to the discussion in related work, several researchers were critical in classifying mass pictures of breast cancer as benign or malignant. Many studies suggested various CNN models with varying parameters and obtained results ranging from 90 to 98%. However, there are other constraints that must be addressed. The major gap in mammography is mass classification using such a model that can categorize it effectively and quickly. It is possible to do this using a hybrid strategy. This study uses the CBIS-DDSM dataset to develop a unique hybrid approach CNN-Inception-V4 for identifying breast cancer masses as benign or malignant.

3. Proposed Methodology

In this research, we developed a novel hybrid strategy for classifying breast cancer as benign or malignant by combining CNN and Inception-V4 networks as showing in Figure 1. The CBIS-DDSM dataset, which contains mammography images, is used in this study. 450 images are utilized for benign, and 450 images are used for malignant. The images are first cleaned by removing pectoral muscles, labels, and white borders. Then, CLAHE is used to these images to improve their quality in order to produce promising classification results.

$$C = C_{\min} + \sqrt{2a^2 \ln \frac{1}{1 - P_{\text{image}}(i)}}, \tag{1}$$

where$C_{\min}$ is the lowest limit of the data point and a_2 is a distribution adjustment factor that is determined for each input picture as showing in Equation (1) [52]. CNN is a form of neural network model that helps us to extract more accurate representations of picture material. Unlike traditional image recognition, which requires you to define the image characteristics, CNN processes the input pixel data from the picture, trains the model, and then extracts the feature representation for better categorization.

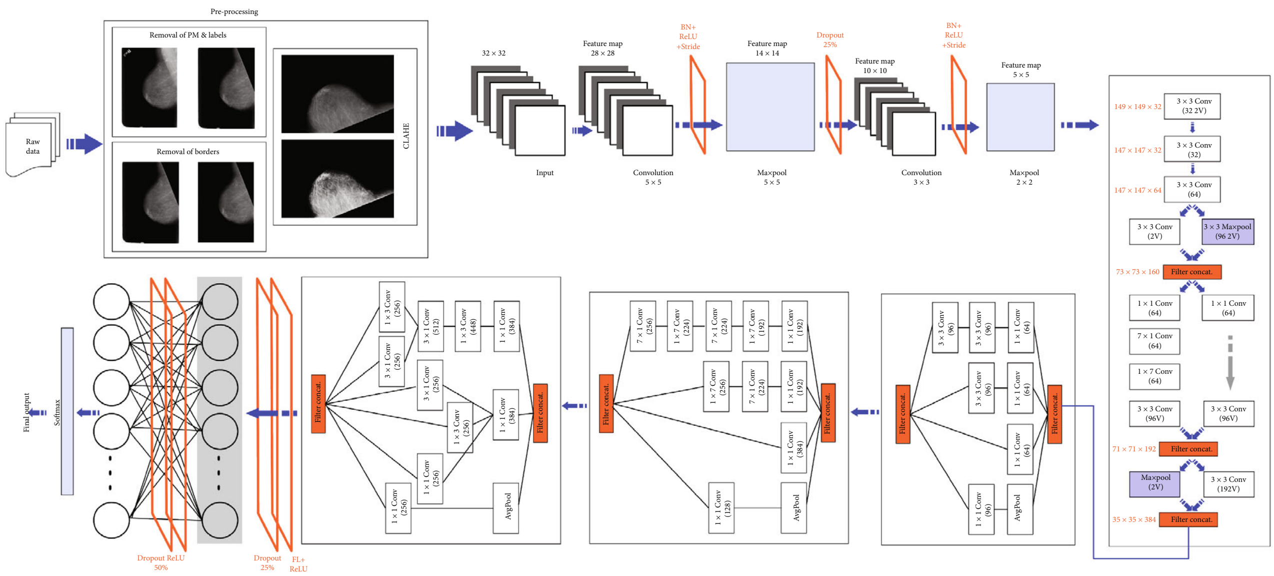

Figure 1: The proposed network with all the steps including preprocessing, network fusion, and then Softmax classification (CNN-Inception-V4 hybrid approach).

Images are cleaned and enhanced before being fed into the hybrid model using filters 32×32.

$$Z = \sum_{i=0}^{0} Z(i)(Z - Zi), \tag{2}$$

where Z is the sequence such that $Z(0) = 1$ as mentioned in Equation (2). Equations (3)–(5) [53] show the impulse response.

$$Y = O(x(t)), \tag{3}$$

$$Y = O\left(\sum_{i=0}^{0} Z(i)(Z - Zi)\right), \tag{4}$$

$$Y = \sum_{i=0}^{0} Z(i)O(Z - Zi). \tag{5}$$

The information is sent to the following stage, which extracts features from Convolution 5×5 (feature map 28×28) using batch normalization [54]+ReLU and stride. A convolution runs the window over pictures and computes the input and filtration system dot product pixel values. This enables convolution to highlight the essential characteristics. The data is then transferred to max pool 5×5 (feature map 14×14) with a 25% dropout rate to extract features more effectively.

$$\begin{Bmatrix} x0 \\ x1 \\ x2 \\ x3 \\ x4 \\ x5 \\ x6 \\ x7 \end{Bmatrix} = \begin{Bmatrix} z0 & 0 & 0 & 0 & 0 & 0 \\ z1 & z0 & 0 & 0 & 0 & 0 \\ z2 & z1 & z0 & 0 & 0 & 0 \\ 0 & z2 & z1 & z0 & 0 & 0 \\ 0 & 0 & z2 & z1 & z0 & 0 \\ 0 & 0 & 0 & z2 & z1 & z0 \\ 0 & 0 & 0 & 0 & z2 & z1 \\ 0 & 0 & 0 & 0 & 0 & z2 \end{Bmatrix} \begin{Bmatrix} y0 \\ y1 \\ y2 \\ y3 \\ y4 \\ y5 \end{Bmatrix}. \tag{6}$$

X is an 8-dimensional vector, Z is a 3-dimensional vector, and y is a 6-dimensional vector. Then, we make an 8×6 matrix that encodes the values of Z so that $X = T(Z)\,y$ as shown in Equation (6). To lower data size and processing time, CNN employs max pooling to replace output with a max summary. This helps you to identify the elements that have the greatest influence while reducing the danger of overfitting. Max pooling takes two hyperparameters into account: stride and size.

$$Ax(t) = \sum_{i=1}^{6} Ay(T)Az(t - T), \tag{7}$$

$$Ax(t) = \sum_{i=0}^{0} Ay(T)Az(t - T), \tag{8}$$

$$Ax(t) = (Ay * Az)(t). \tag{9}$$

Even in this discrete example, the cumulative distribution

Table 1: Testing and training images of benign and malignant.

	Training	Testing
Benign	380	70
Malignant	380	70

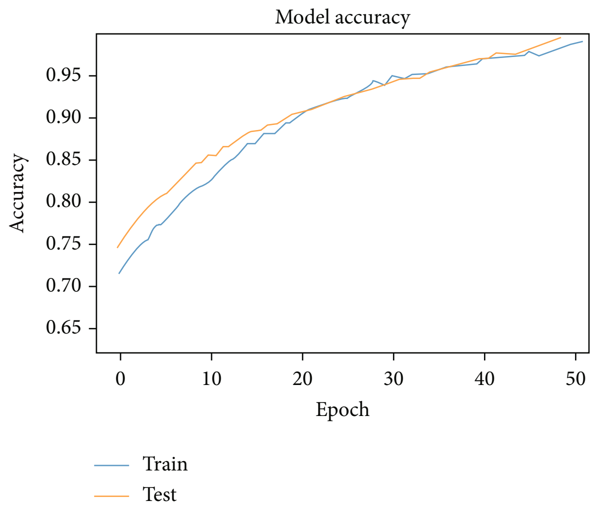

Figure 2: Accuracy graph of training and testing of CNN-Inception-V4.

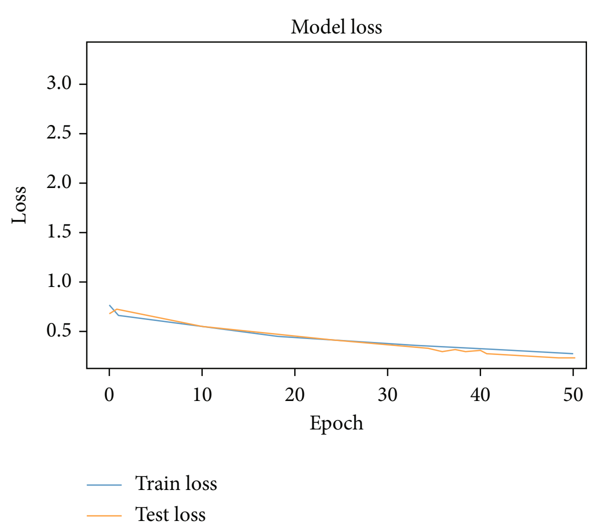

Figure 3: Loss graph of training and testing of CNN-Inception-V4.

functions of$X$, Y, and Z (also known as expected values) are shown in Equations (7)–(9) [52]. The stride determines the skipping of value pools, whereas the length determines the amount of the value pools in each skip. The collected features are then fed into a convolution of 3×3 with 10×10 feature map with batch normalization+ReLU and stride. The results of the convolution layer was then routed to a max pool layer of 2×2 with a 5×5 feature map. Inception-V4 is the result of the merger of various networks.

Inception-v4 is a convolutional neural network structure that improves on prior generations of the Inception family by simplifying the design and employing additional inception modules than Inception-v3. Inception-v4, which evolved from GoogLeNet/Inception-v1, has a more consistent streamlined design and more inception modules than Inception-v3. This network has numerous blocks, including the Stem block, Inception-A block, Inception-B block, and Inception-C block, as well as reduction blocks.

The first block is the stem of the Inception V4 network, in which input is transmitted to a convolution of 32 2 V filters with $149 \times 149 \times 32$ size, then to 3×3 convolution with $147 \times 147 \times 32$ size, and finally to $147 \times 147 \times 64$ with convolution of 64 kernels.

$$yA_{xy} = \sum_{u=1}^{l} \sum_{f=1}^{l} J_{uf} b_{i(x,u),j(y,f)}. \tag{10}$$

Another image matrix A is the convolution of the image b with the kernel J as shown in Equation (10). It then splits into two branches. The first is the max pooling branch, which has 96 2 V, and the second is the 3×3 convolution branch, which has 2 V. The output of these two branches is $73 \times 73 \times 160$ in size. Then, it splits into two branches once more. The first is 1×1 convolution (64), while the second is1×1convolution (64). The first branch advances to various convolution layers, including 7×1 convolution (64), 7×1 convolution (64), and 3×3 convolution (96 V). The second branch goes to 3×3 convolution (96 V). The output is concatenated once again with $71 \times 71 \times 192$ dimensions. Following that, it separates into two branches once more. The first is max pool with a voltage of 2 V, and the second is 3×3 convolution with a voltage of 192 V, and the output from these two branches concatenates to a $35 \times 35 \times 384$ size. The following block is Inception-A, in which the output from the stem is sent into the Inception-A block through the concatenation function. Then, it proceeds to four branches. The first is 1×1 convolution (64), the second is 1×1 convolution (96), and the fourth is AvgPooling. The input from the first branch is routed to 3×3 convolution with 96 and then to 3×3 convolution (96). The input from the second branch is routed to 3×3 convolution (96), while the input from the fourth branch is sent to 1×1 convolution (96). Then, using the filter concatenation function, all inputs from subbranches are concatenated. The input from this block is sent to the Inception-B block, which also contains branches and subbranches as shown in Equations (11)–(14). Input passes to 1×7 convolution (192) from the first branch 1×1 convolution (192), then to 7×1 convolution (224), then to 1×7 convolution (224), and and finally to convolution (256). From the second branch, the input is sent to 1×1 convolution (192), then to 7×1 convolution (224), and finally to convolution (256). 1×1 convolution is the third branch (384).

$$T(A = G) = T(I + J = G), \tag{11}$$

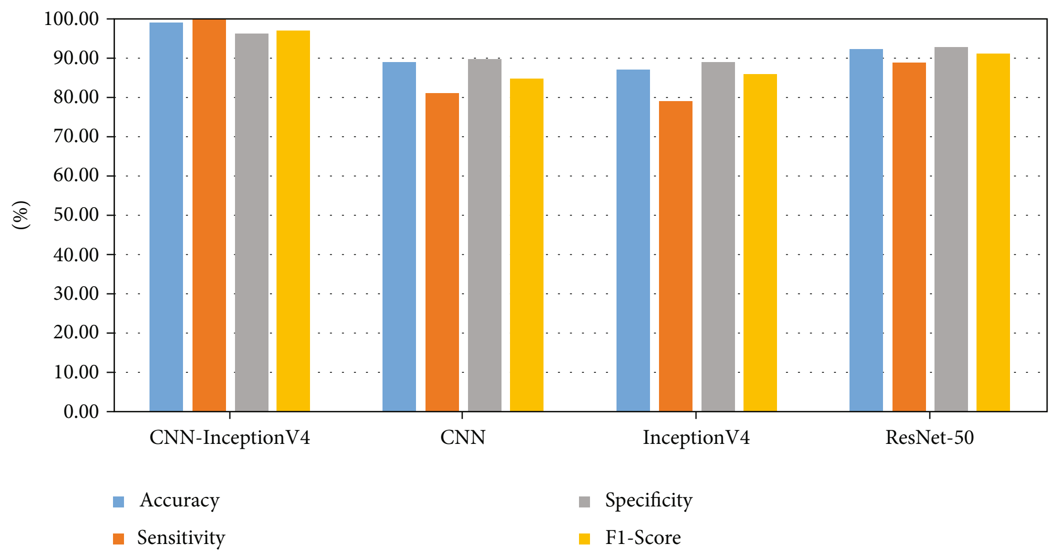

Figure 4: Comparison between our proposed model, CNN, Inception-V4, and ResNet-50 on the basis of accuracy, sensitivity, specificity, and F1-score.

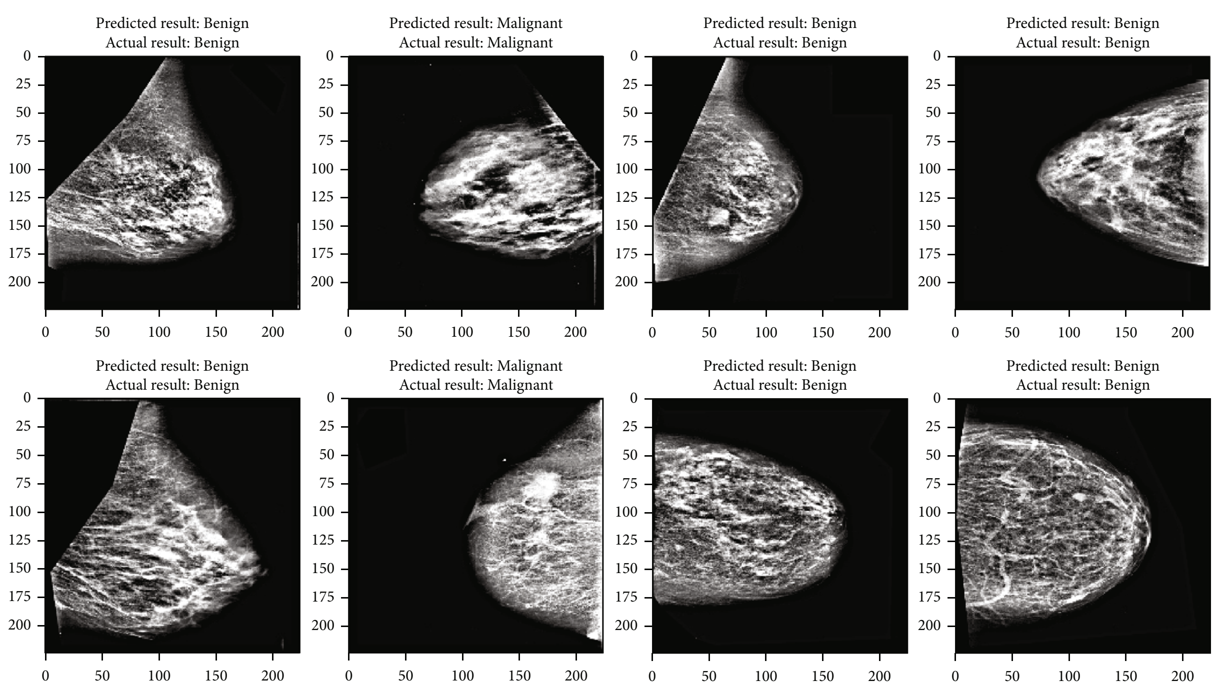

Figure 5: The results showing the actual and predicted values of benign and malignant.

$$T(A = G) = \sum_{u=1}^{6} T(I + J = G \mid J = u)T(J = u), \tag{12}$$

$$T(A = G) = \sum_{u=1}^{6} T(I + u = G)T(J = u), \tag{13}$$

$$T(A = G) = \sum_{u=1}^{6} T(J = u)T(I = G - u). \tag{14}$$

The input from this block is sent to the Inception-B block, which also contains branches and subbranches as showing in Equations (11)–(14). Input passes to 1×7 convolution (192) from the first branch 1×1 convolution (192), then to 7×1 convolution (224), then to 1×7 convolution (224), and finally to convolution (256). From the second branch, the input is sent to 1×1 convolution (192), then to 7×1 convolution (224), and finally to convolution (256). 1×1 convolution is the third branch (384). Input is sent to 1×1 convolution from the fourth branch of

AvgPooling (128). Then, using the filter concatenation function, all inputs from subbranches are concatenated. The following block is Inception-C. The input is routed through multiple branches and subbranches in this block. From the first branch, 1×1 convolution (384), input is passed to 1×3 convolution (448), then to 3×1 convolution (512), then to 1×3 convolution (256), and finally to 3×1 convolution (256). 1×1 convolution (384), 3×1 convolution (256), 1×3 convolution (256), and finally to convolution (256). Input is sent to 1×1 convolution from the third branch of AvgPooling (256). Then, using the filter concatenation function, all inputs from subbranches are concatenated. After going through CNN and the Inception model, the input enters the classification phase, which has a 25% dropout rate and a ReLU activation function.

After passing through classification neurons, it employs Softmax for binary classification and then predicts benign and aggressive breast cancer. This suggested network was trained and tested using 50 epochs and 32 batch sizes, yielding encouraging findings that are reported in the next section.

4. Results and Discussion

In this study, we used the CBIS-DDSM dataset to classify breast cancer as benign or malignant. And, as described in Proposed Methodology, we employed a CNN-Inception-V4 hybrid methodology for this purpose. 450 images are employed for benign, and 450 images are used for malignant.

Testing and training images of benign and malignant are shown in Table 1.

50 epochs and 32 batch size for training and testing are used. We utilized accuracy, sensitivity [55], specificity, and F-score [55] as evaluation metrics. Accuracy is the overall prediction of model as shown in the following equation:

$$\text{Accuracy} = \frac{\text{TP} + \text{TN}}{\text{TP} + \text{TN} + \text{FP} + \text{FN}}. \tag{15}$$

Sensitivity is defined as the proportion of accurately identified real positives as shown in the following equation:

$$\text{Sensitivity} = \frac{\text{TP}}{\text{TP} + \text{FN}}. \tag{16}$$

Specificity is defined as the proportion of accurately identified real negatives as shown in the following equation:

$$\text{Specificity} = \frac{\text{TN}}{\text{TN} + \text{FP}}. \tag{17}$$

The F1-score is a mix of the model's accuracy and recall as shown in the following equation:

$$\text{F1-score} = \frac{2\text{TP}}{2\text{TP} + \text{FN} + \text{FP}}. \tag{18}$$

Our suggested model's accuracy is 99.2%, with a sensitivity of 99.8%, specificity of 96.3%, and F1-score of 97%. We compared our proposed model with CNN, Inception-V4, and ResNet-50. Our proposed model outperforms existing classification models, according to the findings as shown in Figure 2. The training and testing accuracy and loss of CNN-Inception-V4 are shown in Figures 3 and 4, respectively. The x-axis shows the number of epochs and the y-axis shows the accuracy for the model. Training results are shown in blue color, and testing results are shown in orange shade.

Our proposed model 99.2% accurately classifies breast cancer into benign and malignant. The results showing actual and predicted values of benign and malignant are shown in Figure 5.

5. Conclusion and Future Work

Many researchers played an important role in the classification of mass images of breast cancer as benign and malignant, but still, mass classification in mammography remains a significant issue, yet it is essential in assisting radiologists in making accurate diagnoses. There is also a need for such a system that can speed up the process of classification of tumors with good results, and this is possible with a unique hybrid technique. So, using the CBIS-DDSM (Curated Breast Imaging Subset of DDSM) dataset, this research provides a novel hybrid approach CNN-Inception-V4 for classifying breast cancer as benign or malignant. The CBIS-DDSM dataset, which comprises mammography images, is employed. 450 images are used for benign, and 450 images are used for malignant. The images are first cleaned by removing pectoral muscles, labels, and white borders. Then, CLAHE is used to these images to improve their quality in order to produce promising classification results. Following preprocessing, our model diagnoses cancer in mammography pictures as benign or malignant abnormalities (MGI). To lower data size and processing time, CNN employs max pooling to replace output with a max summary. This helps you to identify the elements that have the greatest influence while reducing the danger of overfitting. 50 epochs and 32 batch size for training and testing are used. We utilized accuracy, sensitivity, specificity, and F-score as evaluation metrics. Our suggested model's accuracy is 99.2%, with a sensitivity of 99.8%, specificity of 96.3%, and F1-score of 97%. We also compared our proposed model to CNN, Inception-V4, and ResNet-50. Our proposed model outperforms existing classification models, according to the outcomes. In our research, we employed mass images. As a result, calcification images can be used for further study in the future.

Data Availability

The data used to support the findings of the study are included within the article.

Conflicts of Interest

The authors declare that they have no conflicts of interest.

Acknowledgments

This research was supported by the Information Systems Department, Faculty of Management Comenius University in Bratislava, Odbojárov 10, 82005 Bratislava 25, Slovakia.

References

[1] L. Dorling, S. Carvalho, J. Allen et al., "Breast cancer risk Genes - Association analysis in more than 113,000 women," *The New England journal of medicine*, vol. 384, no. 5, pp. 428–439, 2021.

[2] S. Abbas, Z. Jalil, A. R. Javed et al., "BCD-WERT: a novel approach for breast cancer detection using whale optimization based efficient features and extremely randomized tree algorithm," *PeerJ Computer Science*, vol. 7, p. e390, 2021.

[3] W. Gao, S. Zhang, J. Guo et al., "Investigation of synthetic relaxometry and diffusion measures in the differentiation of benign and malignant breast lesions as compared to BI-RADS," *Journal of Magnetic Resonance Imaging*, vol. 53, no. 4, pp. 1118–1127, 2021.

[4] K. Kerlikowske, S. Chen, M. K. Golmakani et al., "Cumulative advanced breast cancer risk prediction model developed in a screening mammography population," *Journal of the National Cancer Institute*, vol. 114, no. 5, pp. 676–685, 2022.

[5] J. T. Schousboe, B. L. Sprague, L. Abraham et al., "Cost-effectiveness of screening mammography beyond age 75 years," *Annals of Internal Medicine*, vol. 175, no. 1, pp. 11–19, 2022.

[6] S. E. Hickman, R. Woitek, E. P. V. Le et al., "Machine learning for workflow applications in screening mammography: systematic review and meta-analysis," *Radiology*, vol. 302, no. 1, pp. 88–104, 2022.

[7] D. A. Wood, S. Kafiabadi, A. Al Busaidi et al., "Deep learning to automate the labelling of head MRI datasets for computer vision applications," *European Radiology*, vol. 32, no. 1, pp. 725–736, 2022.

[8] A. R. Javed, R. Faheem, M. Asim, T. Baker, and M. O. Beg, "A smartphone sensors-based personalized human activity recognition system for sustainable smart cities," *Sustainable Cities and Society*, vol. 71, p. 102970, 2021.

[9] G. Kantor, V. Niarchos, and C. Papageorgakis, "Solving conformal field theories with artificial intelligence," 2021, http://arxiv.org/abs/2108.08859.

[10] A. R. Javed, M. U. Sarwar, H. U. Khan, Y. D. Al-Otaibi, and W. S. Alnumay, "Pp-spa: privacy preserved smartphone-based personal assistant to improve routine life functioning of cognitive impaired individuals," *Neural Processing Letters*, pp. 1–18, 2021.

[11] A. R. Javed, M. U. Sarwar, M. O. Beg, M. Asim, T. Baker, and H. Tawfik, "A collaborative healthcare framework for shared healthcare plan with ambient intelligence," *Human-centric Computing and Information Sciences*, vol. 10, no. 1, pp. 1–21, 2020.

[12] F. Akram, D. Liu, P. Zhao, N. Kryvinska, S. Abbas, and M. Rizwan, "Trustworthy intrusion detection in e-healthcare systems," *Frontiers in public health*, vol. 9, 2021.

[13] G. Thippa Reddy, A. Srivatsava, K. Lakshmanna, R. Kaluri, S. Karnam, and G. Nagaraja, "Risk prediction to examine health status with real and synthetic datasets," *Biomedical and Pharmacology Journal*, vol. 10, no. 4, pp. 1897–1903, 2017.

[14] T. M. Ali, A. Nawaz, A. U. Rehman et al., "A sequential machine learning-cum-attention mechanism for effective segmentation of brain tumor. front," *Oncol*, vol. 12, p. 873268, 2022.

[15] S. U. Rehman, A. R. Javed, M. U. Khan, M. N. Awan, A. Farukh, and A. Hussien, "Personalisedcomfort: a personalised thermal comfort model to predict thermal sensation votes for smart building residents," *Enterprise Information Systems*, pp. 1–23, 2020.

[16] M. U. Sarwar and A. R. Javed, "Collaborative health care plan through crowdsource data using ambient application," in *2019 22nd international multitopic conference (INMIC)*, pp. 1–6, IEEE, 2019.

[17] A. Priyanka, M. Parimala, K. Sudheer, R. Kaluri, K. Lakshmanna, and M. P. K. Reddy, "Big data based on healthcare analysis using IoT devices," in *IOP Conference Series: Materials Science and Engineering*, vol. 263, IOP Publishing, p. 042059, 2017.

[18] M. K. Hasan, S. Islam, I. Memon et al., "A novel resource oriented DMA framework for Internet of Medical Things devices in 5G network," *IEEE Transactions on Industrial Informatics*, p. 1, 2022.

[19] J. Shi, A. Vakanski, M. Xian, J. Ding, and C. Ning, "EMT-NET: efficient multitask network for computer-aided diagnosis of breast cancer," 2022, http://arxiv.org/abs/2201.04795.

[20] M. Mehmood, M. Rizwan, S. Abbas et al., "Machine learning assisted cervical cancer detection," *Frontiers in public health*, vol. 9, 2021.

[21] A. R. Javed, L. G. Fahad, A. A. Farhan et al., "Automated cognitive health assessment in smart homes using machine learning," *Sustainable Cities and Society*, vol. 65, p. 102572, 2021.

[22] M. Rizwan, A. Shabbir, A. R. Javed et al., "Risk monitoring strategy for confidentiality of healthcare information," *Computers and Electrical Engineering*, vol. 100, p. 107833, 2022.

[23] S. Bhattacharya, S. R. K. Somayaji, T. R. Gadekallu, M. Alazab, and P. K. R. Maddikunta, "A review on deep learning for future smart cities," *Internet Technology Letters*, vol. 5, no. 1, p. e187, 2022.

[24] A. R. Javed, M. U. Sarwar, S. Khan, C. Iwendi, M. Mittal, and N. Kumar, "Analyzing the effectiveness and contribution of each axis of tri-axial accelerometer sensor for accurate activity recognition," *Sensors*, vol. 20, no. 8, p. 2216, 2020.

[25] N. Tomasev, I. Bica, B. McWilliams et al., "Pushing the limits of self-supervised ResNets: can we outperform supervised learning without labels on ImageNet?," 2022, http://arxiv.org/abs/2201.05119.

[26] S. Safdar, M. Rizwan, T. R. Gadekallu et al., "Bio-imaging-based machine learning algorithm for breast cancer detection," *Diagnostics*, vol. 12, no. 5, p. 1134, 2022.

[27] A. Mohiyuddin, A. Basharat, U. Ghani et al., "Breast tumor detection and classification in mammogram images using modified YOLOv5 network," *Computational and Mathematical Methods in Medicine*, vol. 2022, Article ID 1359019, 16 pages, 2022.

[28] M. M. Alshammari, A. Almuhanna, and J. Alhiyafi, “Mammography image-based diagnosis of breast cancer using machine learning: a pilot study,” *Sensors*, vol. 22, no. 1, p. 203, 2022.

[29] M. K. Hasan, T. M. Ghazal, A. Alkhalifah et al., “Fischer linear discrimination and quadratic discrimination analysis–based data mining technique for internet of things framework for healthcare,” *Frontiers in Public Health*, vol. 9, 2021.

[30] M. K. Hasan, A. Md, S. Rayhan Kabir et al., “Evolution of industry and blockchain era: monitoring price hike and corruption using BIoT for smart government and Industry 4.0,” *IEEE Transactions on Industrial Informatics*, 2022.

[31] M. K. Hasan, M. M. Ahmed, A. H. A. Hashim, A. Razzaque, S. Islam, and B. Pandey, “A novel artificial intelligence based timing synchronization scheme for smart grid applications,” *Wireless Personal Communications*, vol. 114, no. 2, pp. 1067–1084, 2020.

[32] M. K. Hasan, S. Islam, R. Sulaiman et al., “Lightweight encryption technique to enhance medical image security on internet of medical things applications,” *IEEE Access*, vol. 9, pp. 47731–47742, 2021.

[33] M. Akhtaruzzaman, M. K. Hasan, S. R. Kabir, S. N. H. S. Abdullah, M. J. Sadeq, and E. Hossain, “HSIC bottleneck based distributed deep learning model for load forecasting in smart grid with a comprehensive survey,” *IEEE Access*, vol. 8, pp. 222977–223008, 2020.

[34] V. S. Gnanasekaran, S. Joypaul, P. M. Sundaram, and D. D. Chairman, “Deep learning algorithm for breast masses classification in mammograms,” *IET Image Processing*, vol. 14, no. 12, pp. 2860–2868, 2020.

[35] E. H. Houssein, M. Hassaballah, I. E. Ibrahim, D. S. AbdElminaam, and Y. M. Wazery, “An automatic arrhythmia classification model based on improved marine predators algorithm and convolutions neural networks,” *Expert Systems with Applications*, vol. 187, p. 115936, 2022.

[36] Q. Lin, W.-M. Tan, S.-Y. Zhu et al., “Deep learning-based microcalcification detection and classification of mammography for diagnosis of breast cancer,” 2022, Available at SSRN 4001825.

[37] B. Swiderski, L. Gielata, P. Olszewski, S. Osowski, and M. Kołodziej, “Deep neural system for supporting tumor recognition of mammograms using modified GAN,” *Expert Systems with Applications*, vol. 164, p. 113968, 2021.

[38] S. M. Samuri, T. V. Nova, B. Rahmatullah, S. L. Wang, and Z. T. Al-Qaysi, “Classification model for breast cancer mammograms,” *IIUM Engineering Journal*, vol. 23, no. 1, pp. 187–199, 2022.

[39] N. S. Ismail and C. Sovuthy, “Breast cancer detection based on deep learning technique,” in *2019 International UNIMAS STEM 12th Engineering Conference (EnCon)*, pp. 89–92, IEEE, 2019.

[40] A. F. Ibrahim, M. Hassaballah, A. A. Ali, Y. Nam, and I. A. Ibrahim, “COVID19 outbreak: a hierarchical framework for user sentiment analysis,” *Computers, Materials, & Continua*, pp. 2507–2524, 2022.

[41] H. K. Mewada, A. V. Patel, M. Hassaballah, M. H. Alkinani, and K. Mahant, “Spectral–spatial features integrated convolution neural network for breast cancer classification,” *Sensors*, vol. 20, no. 17, p. 4747, 2020.

[42] A. Pillai, A. Nizam, M. Joshee, A. Pinto, and S. Chavan, “Breast cancer detection in mammograms using deep learning,” in *Applied Information Processing Systems*, pp. 121–127, Springer, 2022.

[43] D. Singh and A. K. Singh, “Role of image thermography in early breast cancer detection-past, present and future,” *Computer methods and programs in biomedicine*, vol. 183, p. 105074, 2020.

[44] S. Hadush, Y. Girmay, A. Sinamo, and G. Hagos, “Breast cancer detection using convolutional neural networks,” 2020, http://arxiv.org/abs/2003.07911.

[45] M. Pavithra, R. Rajmohan, T. A. Kumar, and R. Ramya, “Prediction and classification of breast cancer using discriminative learning models and techniques,” in *Machine Vision Inspection Systems*, vol. Volume 2, pp. 241–262, Machine Learning-Based Approaches, 2021.

[46] Y.-D. Zhang, S. C. Satapathy, D. S. Guttery, J. M. Gorriz, and S.-H. Wang, “Improved breast cancer classification through combining graph convolutional network and convolutional neural network,” *Information Processing & Management*, vol. 58, no. 2, p. 102439, 2021.

[47] S. Annamalai, R. Udendhran, and M. Balamurgan, “Hybridized neural network and decision tree based classifier for prognostic decision making in breast cancers,” *Soft Computing*, vol. 24, no. 11, pp. 7947–7953, 2020.

[48] R. K. Samala, H.-P. Chan, L. M. Hadjiiski, M. A. Helvie, and C. D. Richter, “Generalization error analysis for deep convolutional neural network with transfer learning in breast cancer diagnosis,” *Physics in Medicine & Biology*, vol. 65, no. 10, p. 105002, 2020.

[49] J. J. Patel and S. K. Hadia, “An enhancement of mammogram images for breast cancer classification using artificial neural networks,” *IAES International Journal of Artificial Intelligence*, vol. 10, no. 2, p. 332, 2021.

[50] M. M. Amalmary and A. Prakash, *Elephant herding optimization with bi-directional long shortterm memory network (EHOBI-LSTM) for breast cancer detection in digital mammograms*.

[51] M. F. EnasEl, “Houby and Nisreen IR Yassin. “Malignant and nonmalignant classification of breast lesions in mammograms using convolutional neural networks”,” *Biomedical Signal Processing and Control*, vol. 70, p. 102954, 2021.

[52] A. M. Reza, “Realization of the contrast limited adaptive histogram equalization (CLAHE) for real-time image enhancement,” *Journal of VLSI signal processing systems for signal, image and video technology*, vol. 38, no. 1, pp. 35–44, 2004.

[53] S. SimaSahu, A. K. Singh, S. P. Ghrera, and M. Elhoseny, “An approach for de-noising and contrast enhancement of retinal fundus image using CLAHE,” *Optics & Laser Technology*, vol. 110, pp. 87–98, 2019.

[54] O. Junghun, H. Kim, S. Baik, C. Hong, and K. M. Lee, “Batch normalization tells you which filter is important,” in *Proceedings of the IEEE/CVF Winter Conference on Applications of Computer Vision*, pp. 2645–2654, 2022.

[55] A. Kovacs, P. Palasti, D. Vereb, B. Bozsik, A. Palkó, and Z. T. Kincses, “The sensitivity and specificity of chest CT in the diagnosis of COVID-19,” *European Radiology*, vol. 31, no. 5, pp. 2819–2824, 2021.